

Microstructure characteristics of laser-MIG hybrid welded 2A12 aluminum alloy joint with titanium addition and heat treatment conditions

J. Yan¹, M. Gao^{2*}, G. Li², C. Zhang², M. Jiang², X. Y. Zeng²

¹*The 9th Overal Design Department of China Aerospace Science & Industry Corp., Wuhan, Hubei 430040, PR China*
²*Wuhan National Laboratory for Optoelectronics, Huazhong University of Science and Technology, Wuhan, Hubei 430074, PR China*

Received 28 June 2012, received in revised form 9 November 2012, accepted 1 August 2013

Abstract

This paper presents the effects of titanium addition and heat treatment on microstructure of 2A12 aluminum alloy joints by CO₂ laser-metal inter gas hybrid welding. The 5 mm thick 2A12 aluminum alloy plates were welded by hybrid welding with and without titanium addition, respectively. The results showed that the oriented columnar dendrites were formed near the fusion boundary without titanium addition. However, the Al₃Ti particles are formed to provide excellent nucleation sites for α -Al grains after titanium addition. Furthermore, a chill zone consisting of fine spherical grains was formed to prevent the growth of columnar dendrites between the base metal and fusion zone. Moreover, the grain size of the chill zone was much smaller than that of the weld center region. After heat treatment, the microstructure transitioned from columnar dendrites to fine equiaxed grains and the eutectics are believed as α -Al₁, θ phases, and some other inclusions.

Key words: laser welding, hybrid welding, aluminum alloy

1. Introduction

Due to the excellent mechanical properties and low density, 2A12 aluminum alloy is used extensively in light weight structures. Arc welding is used to make aluminum structures. However, owing to the low welding speed and high heat input, the coarse grains are formed seriously in the heat affected zone (HAZ), and the joint strength is very low. Laser beam welding is used extensively in industrial applications for steel welding. However, it is difficult to weld the aluminum alloy because of its high reflectivity and the vaporization of low boiling point alloying elements. Some welding defects such as cracks and porosities are easily formed, which represent a great challenge to designers and technologists [1, 2]. As a new fusion welding method, the laser-metal inter gas (MIG) hybrid welding integrates laser beam and electric arc. Advantages of hybrid welding process include higher welding stability, higher melting efficiency, easier addition of welding wires and lower power input under the same

welding penetration [3]. The hybrid welding method is considered to be suitable for aluminum alloy and the joint strength can be increased in some extent owing to its high welding speed and low heat input when compared to traditional arc welding methods. Due to the rapid cooling rates associated with hybrid welding, dendrite crystals and low melting eutectic should be formed in fusion zone unavoidable, which results in inferior mechanical properties and high crack sensitivity [4].

In recent years, great deals of efforts have been devoted to improve the joint strength. The heat treatment is a traditional method to improve the joint strength, and the use of grain refiners is a regular practice for further enhancement of the joint properties. Solution and aging treatment are effective to modify the precipitates segregation and large columnar grains in welds, which are formed in welding process. Elangovan had found that there was a significant variation in the size and distribution of strengthening particles about 6061 friction stir welding joint after

*Corresponding author: tel.: +86 27 87792404; fax: +86 27 87541423; e-mail address: mgao@mail.hust.edu.cn

Table 1. Chemical composition of parent material and welding wires, wt.%

Composition	Si	Cu	Mg	Mn	Fe	Ti	Zn	Al
Parent material	0.5	3.8–4.9	1.2–1.8	0.3–0.9	0.5	0.15	0.25	Bal.
ER2319	0.2	5.8–6.8	0.02	0.2–0.4	0.3	0.2	0.1	

post weld heat treated [5]. Malarvizhi and Aydin investigated the influence of post weld heat treatment on fatigue crack growth behavior of electron beam welded AA2219 alloy and tensile properties of friction stir welded 2024 alloys [1, 6]. However, it had been reported seldom about the effect of heat treatment on various microstructures for 2A12 aluminum alloy joint by laser-MIG hybrid welding.

It is common practice to add titanium to aluminum alloys because of its potential grain refining effects, and the Al_3Ti precipitation phases can be formed. The beneficial effects of titanium additions on the fusion zone grain structure and wear properties of Al-Si eutectic alloys have been studied by Laoui et al. [7]. Moreover, the influence of titanium addition on the microstructure and hardness properties of near-eutectic Al-Si alloys has been investigated in detail by Zeren [8]. However, not much work has been reported on the grain refinement of 2A12 aluminum alloys. Especially, few reports can be found about the effect of titanium addition on microstructure of 2A12 aluminum alloy joints by laser-MIG hybrid welding.

In this study, the 5 mm thick 2A12 aluminum alloy plates were welded by CO_2 laser-MIG arc hybrid welding with and without titanium additions. Post weld solution heat treatment was conducted. The optic and scanning electron microscopy were used to study the microstructure characteristics and segregation behavior of major alloying elements. The contents of Cu, Fe, Mn and Al within eutectics were obtained by energy dispersive X-ray spectroscopy (EDS) and ZAF software. Finally, the effect of titanium addition and heat treatment on microstructures is discussed in detail.

2. Experimental

A 5 kW Rofin TR050 CO_2 laser and a Panasonic 350A conventional DCEP MIG welder were used in the experiments. A welding head combining a CO_2 laser beam and a MIG torch was developed. This system is schematically shown in Fig. 1 [9]. The 5 mm thick 2A12 aluminum alloy plates and commercial ER2319 welding wires were used in the experiments. The nominal chemical composition of the substrate and welding wires are listed in Table 1. Sheared edges were applied for the butt-welding. The surface of the plates was cleaned, degreased and dried before the welding. The experiments were done with the titanium

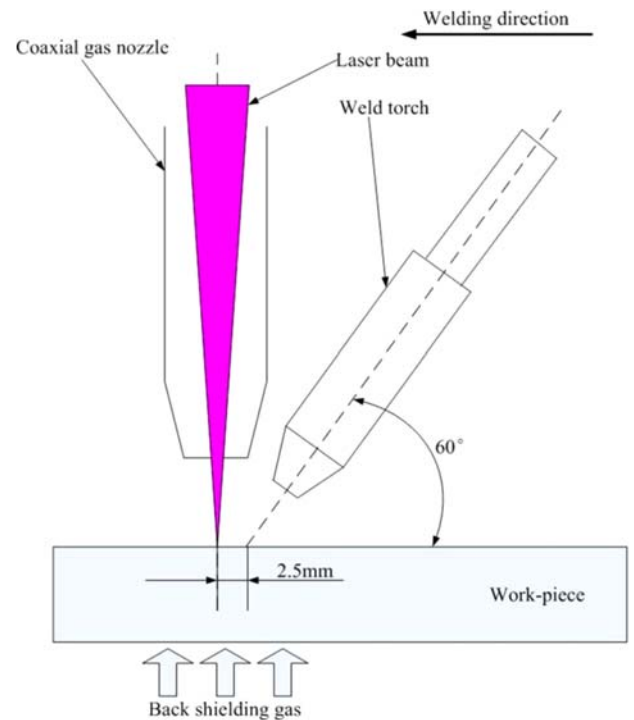


Fig. 1. Schematic diagram of CO_2 laser-MIG hybrid welding.

Table 2. Experimental set-up and parameters

Welding parameters	Value
Beam wave length (μm)	10.6
Focus spot diameter (mm)	0.6
Focal length of lens (mm)	300
Unfocused length (mm)	-2
Wire extension length (mm)	14
Wire diameter (mm)	1.6
Coaxial gas nozzle pure He (L min^{-1})	7.5
MIG torch nozzle pure Ar (L min^{-1})	15
Welding current (A)	120
Welding voltage (V)	20
Welding rate (m min^{-1})	0.8
Laser power (kW)	3.5

powder pre-placed on the surface of the base material. The optimal welding parameters shown in Table 2 were chosen to achieve full penetration. For metallographic examination, fusion zone specimens were

etched with Keller's reagent. For post-welding solution heat treatment, weld samples were immersed in a salt bath at 490°C for 25 min, then immediately quenched in water to room temperature. For natural aging treatment, the samples were placed in air and the aging time was more than 96 h. The optical microscopy was conducted to study the microstructure of joints, and the distribution of main alloy elements was obtained by map scanning analysis. The scanning electron microscopy (SEM) micrographs were conducted to obtain secondary electron images and back-scattered electron (BSE) images. The contents of Cu, Mg, Si and Al were obtained by energy dispersive X-ray spectroscopy (EDS) and ZAF software.

3. Results and discussion

3.1. Microstructure of joints without titanium addition

Optical micrograph of the 2A12 aluminum alloy is shown in Fig. 2. The microstructure consists of α -Al

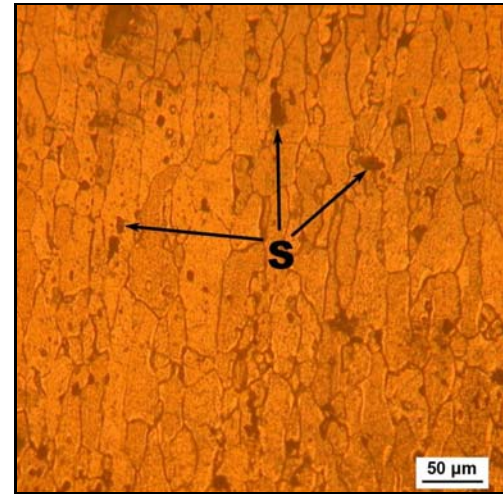


Fig. 2. Microstructure of 2A12-T4 aluminum alloy.

matrix and additional S and minimum θ particles [10, 11]. 5 mm sheets were successfully processed by CO₂ laser-MIG hybrid welding and no superficial porosity

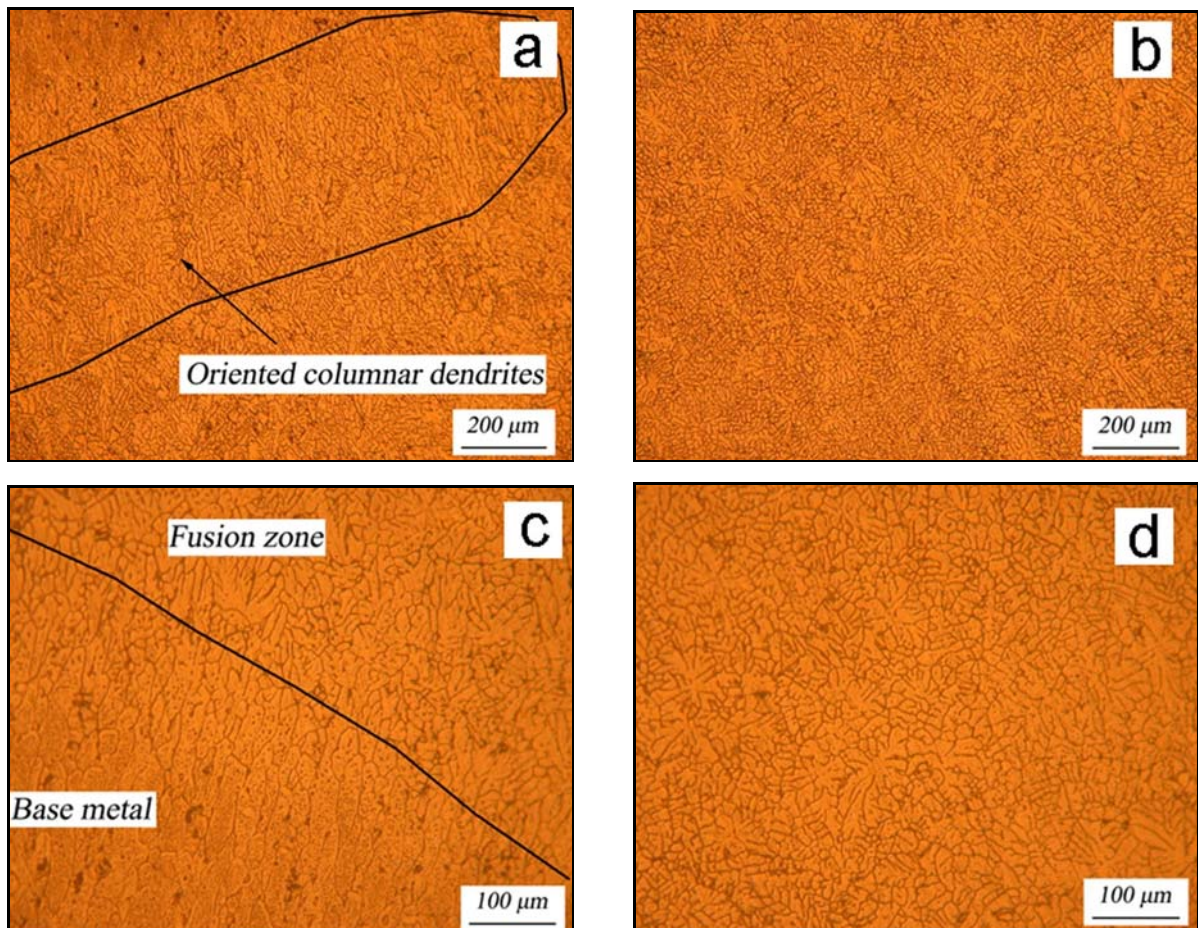


Fig. 3a–d. Microstructure of joint without titanium addition.

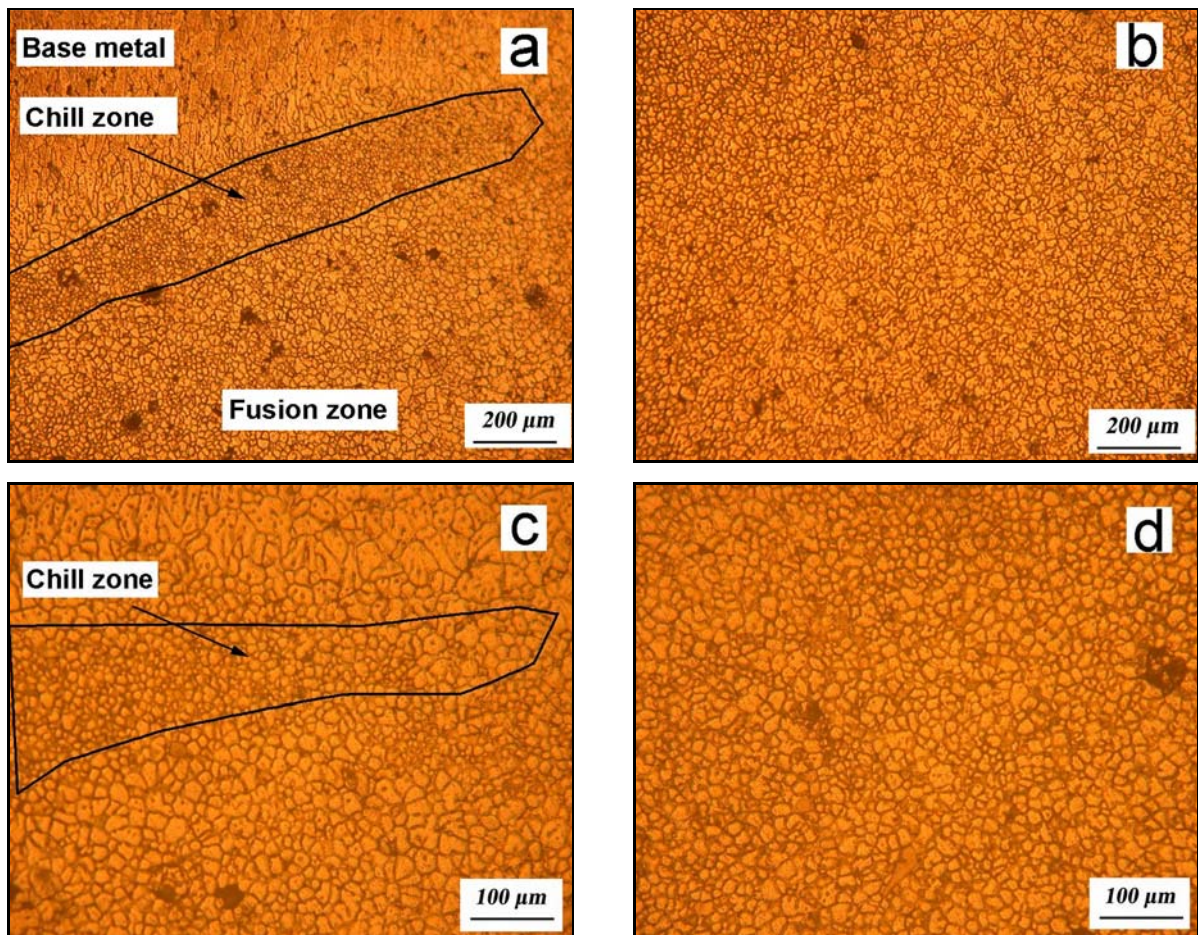


Fig. 4a–d. Microstructure of joint with titanium addition.

or defects were observed in both top and rear surface. Figure 3 shows the typical optical microstructure of joint without titanium additions. The oriented columnar dendrites (shown in Fig. 3a) extended from the fusion boundary to the joint centerline. The columnar zones were formed because the partially melted grains along the fusion boundary provided excellent nucleation sites for the growth of grains and the epitaxial growth results in long and oriented columnar grains under high thermal gradient conditions [12]. Figure 3b shows the predominantly continuous network dendrites structure in the joint center. Furthermore, there is no obvious (shown in Fig. 3c) HAZ in the fusion boundary because of high welding speed and low heat input in the hybrid welding. Additionally, the well distributed dendrites in the joint center can be observed very clearly in Fig. 3d.

3.2. Microstructure of joints with titanium addition

Figure 4 shows the typical optical microstructure of the joint with titanium additions. It can be observed that a chill zone is formed between the base metal and

fusion zone. The chill zone consists of near spherical equiaxed grains and it prevents the growth of columnar dendrites [13–17]. The formation of chill zone can be explained as follows: there exists a thin solid/liquid layer near the fusion boundary, which has a composition similar to that of the base metal and the temperature is just sufficient for recrystallization. However, the additional titanium gathers in solid/liquid interface forward, which results in constitutional supercooling. As welding of aluminum alloys is a rapid cooling process, the further grain growth is not taking place, and hence the grains are much finer in that region [18, 19].

Furthermore, the metallographic examination (shown in Fig. 4) reveals that the columnar solidification structure is suppressed while the fine equiaxed grains are formed. It can be explained as follows: Figure 5 shows the map scanning analysis in the fusion zone of joint with titanium addition. It reveals the dark intercellular phases rich in Cu scattered at grain boundary, but the titanium distributed uniformly in the fusion zone, which represents the titaniferous compounds (Al_3Ti) distributed uniformly. Because of the lower solubility in $\alpha\text{-Al}$ matrix, the partially melted

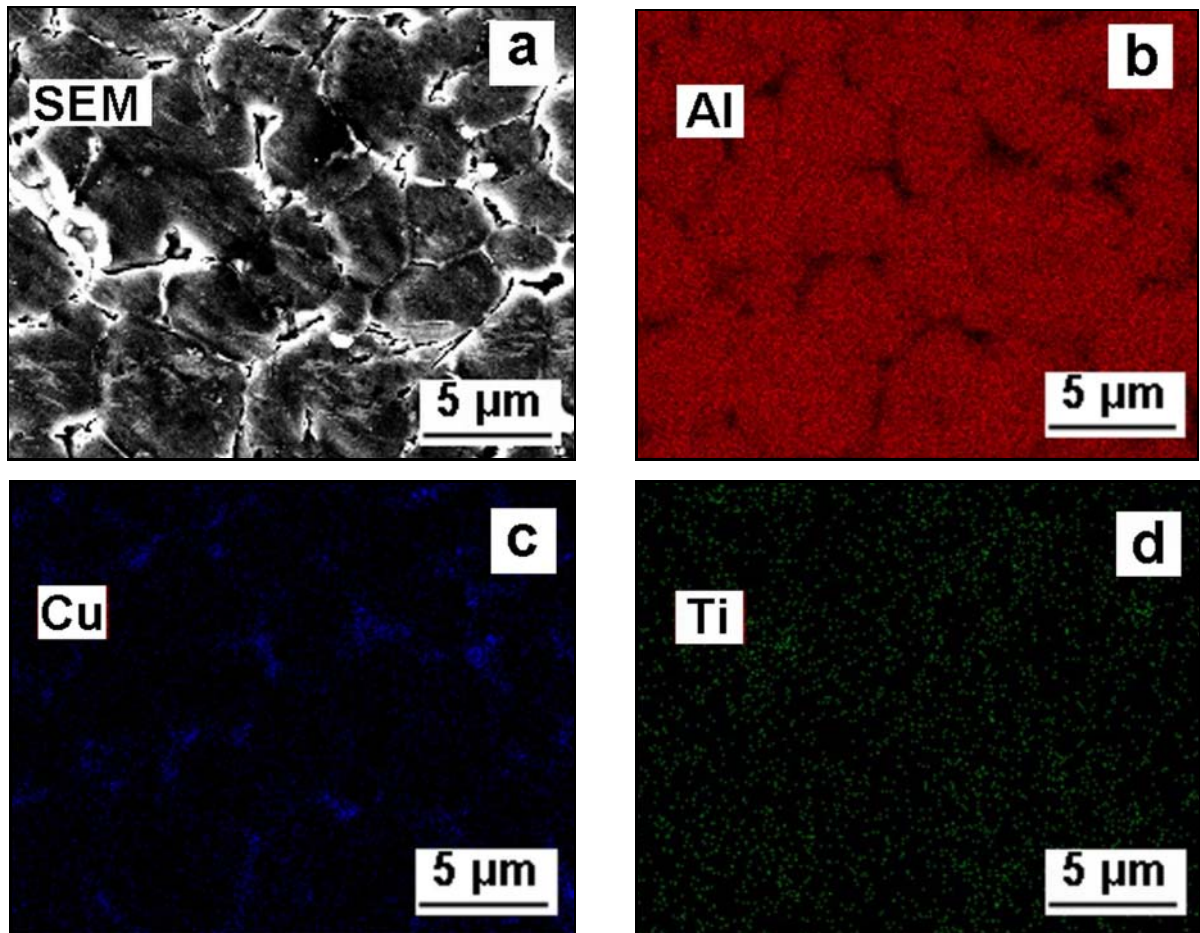


Fig. 5a–d. Map scanning analysis of joint with titanium addition.

Al_3Ti particles having low lattice mismatch with $\alpha\text{-Al}$ results in low interfacial energy between the substrate and nucleated phase. Thus, the Al_3Ti particles serve as heterogeneous nucleation sites for the growth of equiaxed grains, and the nucleation sites have not enough time to grow, which results in fine equiaxed grains during solidification [18].

In addition, there is a noticeable variation in the grain size between the chill zone and the weld centre zone, which can be demonstrated clearly in Fig. 4c,d. The average grain size of the chill zone is much smaller than that of the weld center zone. The different grain size and microstructure morphology in the chill zone and weld center regions are attributed to different cooling conditions. The temperature gradient (G) and the solidification rate (R) affect the solidification behavior and final microstructure of the weld pool. As the value of G/R increases, the interface morphology changes from equiaxed dendrites to cellular grains. Due to the higher cooling rate in the chill zone region when compared with that in the weld center region, higher temperature gradient in the chill zone led to higher G/R value and the equiaxed spherical grain formed, while in the weld center, the value of G/R was

decreased and the equiaxed dendrites occurred [20].

3.3. Microstructure of joints after heat treatment

Standard heat treatment on the joints was performed using the procedure described above. Figure 6 shows the microstructure of the joint after solution heat treatment. Compared with the images shown in Fig. 3, the microstructures changed from the dendritic structure to the spheroidal grains [4]. In addition, it can be observed that a spot of eutectics retain at grain boundaries after heat treatment. Figure 6c,d present much higher magnification micrographs to show the morphology of eutectics at grain boundaries. The eutectics exist as polygonal and honeycomb morphology. Figure 7 exhibits the chemical composition of two randomly chosen locations by the EDS analysis. P1 and P2 zones denote the eutectic at grain boundaries and the precipitates within $\alpha\text{-Al}$ matrix, respectively. The results demonstrate that the two zones contain higher concentrations of Cu than the surrounding matrix material. The eutectics are believed as $\alpha\text{-Al}$, θ phases and some other inclusions. Furthermore, it

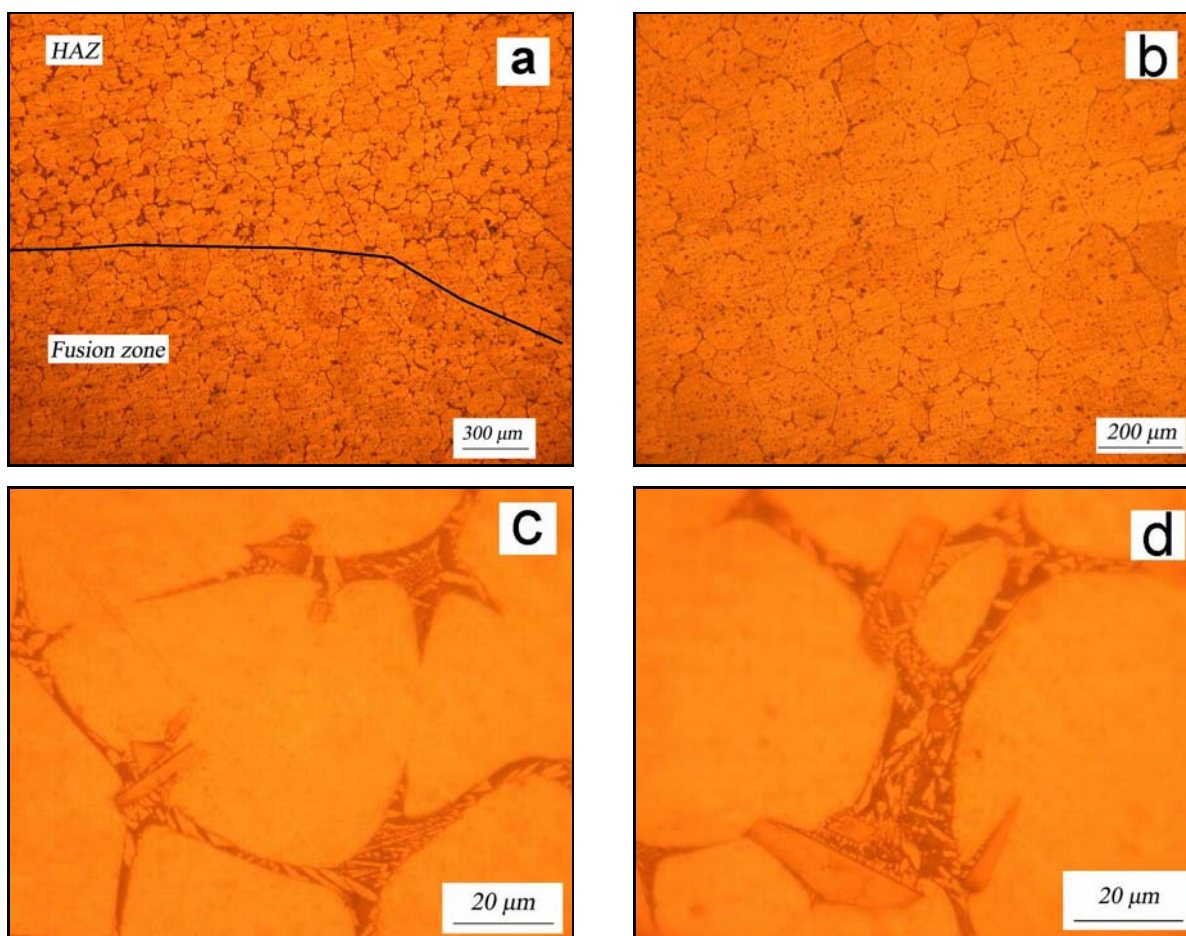


Fig. 6a–d. Microstructure of joints after solution heat treatment.

should be noted that the inclusions are rich in Mn and Fe.

Precipitate strengthened alloys show a decrease of mechanical properties in the weld zone because of the dissolution and growth of strengthening precipitates during the welding thermal cycle. Homogenization heat treatment of the welded samples is a logical solution to eliminate the alloying micro-segregation and to improve the weld hardness. The whole microstructure evolution process consists of three stages [21]. First, the eutectics melt and the primary dendritic grains coarsen into interconnected non-dendritic grains, and recrystallization occurs. Secondly, the eutectics melt along the primary α -Al and the recrystallized grain boundaries, and the new recrystallized grains combine and grow. Finally, the grains become separated from each other and spheroidized at the heat treatment temperature range. In a word, the eutectic phases dissolve completely and alloy elements distribute uniformly during the solution heat treatment. After the quenching treatment, supersaturated solid solution is formed. The long exposure in air during the artificially aged process promotes the atoms diffusion. At last, the θ phases precipitate within grains and at

grain boundaries from the supersaturated α -Al matrix. Thus, there are massive precipitates within grains and a small amount of eutectics re-precipitate at grain boundaries.

4. Conclusions

The 5 mm thick 2A12 aluminum alloy plates were welded by CO₂ laser-MIG hybrid welding with and without titanium addition. Full penetration welds without any defects were produced. The microstructure characteristics of the joints were studied. The following conclusions were derived from the above experimental results and discussion.

1. Without titanium addition, the oriented columnar dendrites and network dendrites were formed near the fusion boundary and joint center, respectively. However, the Al₃Ti particles are formed to provide excellent nucleation sites for α -Al grains in the joint after titanium addition.

2. With titanium addition, a chill zone consisting of fine spherical grains was formed to prevent the growth of columnar dendrites between the base metal and fu-

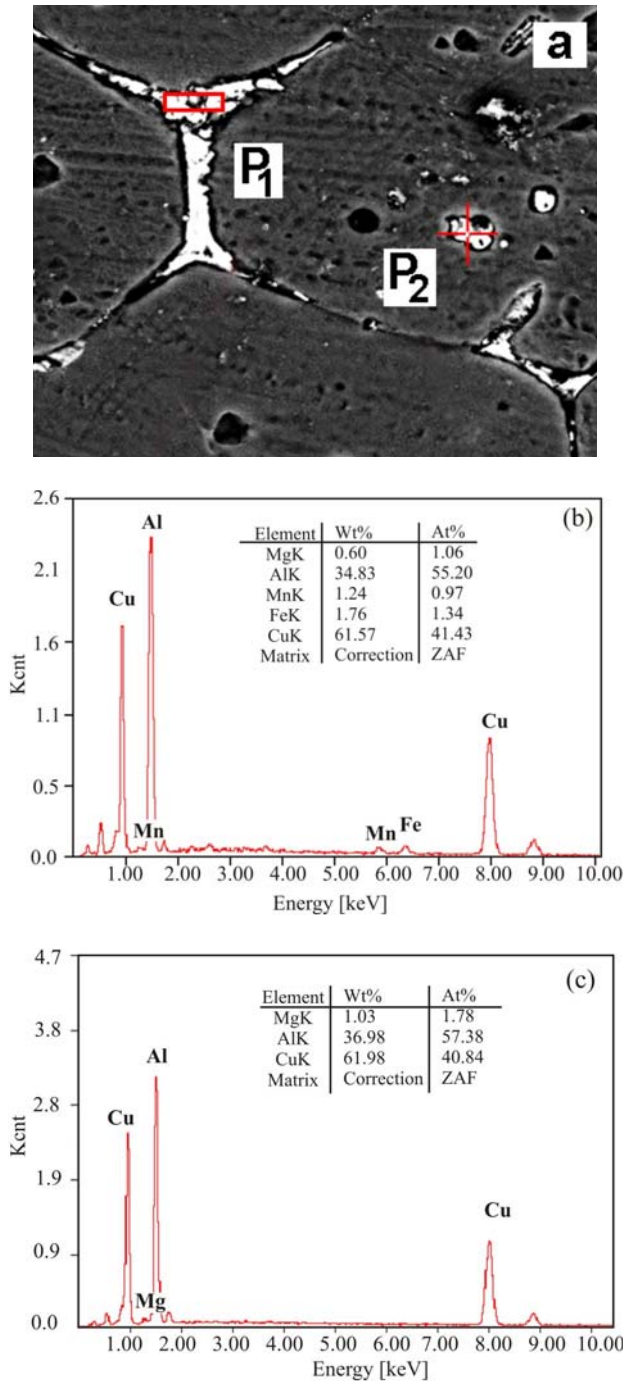


Fig. 7. SEM photographs (a) for EDS analysis (b) and (c).

sion zone. Moreover, the grain size of the chill zone was much smaller than that of the weld center region.

3. The microstructure transitioned from columnar dendrites to fine equiaxed grains after heat treatment. Moreover, the eutectics existing as polygonal and honeycomb morphology retained at grain boundaries. The eutectics are believed as α -Al, θ phases and some other inclusions, which are rich in Mn and Fe.

Acknowledgements

The authors gratefully acknowledge the financial support by the China Postdoctoral Science Foundation with grant No. 2012M521422 and National Natural Science Foundation of China (NSFC) with grant No. 51275186.

References

- [1] Aydin, H., Bayram, A., Uguz, A., Akay, K. S.: *Mater. Des.*, **30**, 2009, p. 2215. [doi:10.1016/j.matdes.2008.08.034](https://doi.org/10.1016/j.matdes.2008.08.034)
- [2] Yeni, C., Sayer, S., Pakdil, M.: *Kovove Mater.*, **47**, 2009, p. 342.
- [3] Gao, M., Zeng, X. Y., Hu, Q. W.: *Sci. Technol. Weld. Join.*, **11**, 2006, p. 520. [doi:10.1179/174329306X148138](https://doi.org/10.1179/174329306X148138)
- [4] Hu, B., Richardson, I. M.: *Mater. Sci. Eng. A*, **459**, 2007, p. 98. [doi:10.1016/j.msea.2006.12.094](https://doi.org/10.1016/j.msea.2006.12.094)
- [5] Elangovana, K., Balasubramanian, V.: *Mater. Charact.*, **59**, 2008, p. 1175.
- [6] Malavizhi, S., Raghukandan, K., Viswanathan, N.: *Int. J. Fatigue*, **30**, 2008, p. 1550. [doi:10.1016/j.ijfatigue.2007.12.002](https://doi.org/10.1016/j.ijfatigue.2007.12.002)
- [7] Saheb, N., Laoui, T., Daud, A. R., Harun, M., Radiman, S., Yahaya, R.: *Wear*, **249**, 2001, p. 660. [doi:10.1016/S0043-1648\(01\)00687-1](https://doi.org/10.1016/S0043-1648(01)00687-1)
- [8] Zeren, M., Karakulak, E.: *J. Alloys Compd.*, **450**, 2008, p. 258. [doi:10.1016/j.jallcom.2006.10.131](https://doi.org/10.1016/j.jallcom.2006.10.131)
- [9] Yan, J., Zeng, X. Y., Gao, M., Lai, J., Lin, T. X.: *Appl. Surf. Sci.*, **255**, 2009, p. 7311.
- [10] Rao, K. S., Reddy, G. M., Rao, K. P.: *Mater. Sci. Eng. A*, **403**, 2005, p. 73.
- [11] Sik, A., Onder, M.: *Kovove Mater.*, **50**, 2012, p. 132.
- [12] Savage, W. F., Nippes, E. F., Erickson, I. S.: *Weld. J.*, **55**, 1976, p. 218.
- [13] Reddy, G. M., Gokhale, A. A., Prasad, K. S., Rao, K. P.: *Sci. Technol. Weld. Join.*, **3**, 1998, p. 210.
- [14] Chang, W. S., Rajesh, S. R., Chun, C. K., Kim, H. J.: *J. Mater. Sci. Technol.*, **27**, 2011, p. 201. [doi:10.1179/174328409X418973](https://doi.org/10.1179/174328409X418973)
- [15] Aidun, D. K., Dean, J. P.: *Weld. J.*, **78**, 1999, p. 350.
- [16] Aroral, K. S., Pandey, S., Schaper, M., Kumar, R.: *J. Mater. Sci. Technol.*, **26**, 2010, p. 750. [doi:10.1179/174328409X405607](https://doi.org/10.1179/174328409X405607)
- [17] Lin, D. C., Wang, G. X., Srivatsan, T. S.: *Mater. Sci. Eng. A*, **351**, 2003, p. 307.
- [18] Dev, S., Stuart, A. A., Murty, B. S., Rao, K. P.: *Mater. Sci. Eng. A*, **467**, 2007, p. 135.
- [19] Fu, G. S., Sun, F. S., Ren, L. Y., Chen, W. Z., Qian, K. W.: *J. Rare Earths*, **20**, 2002, p. 64.
- [20] Aval, H. J., Farzadi, A., Serajzadeh, S., Kokabi, A. H.: *Int. J. Adv. Manuf. Technol.*, **42**, 2009, p. 1048.
- [21] Wang, J. G., Lu, P., Wang, H. Y., Liu, J. F., Jiang, Q. C.: *J. Alloys Compd.*, **395**, 2005, p. 110.